Richter and Schicker *Journal of Statistical Distributions and Applications* (2017) 4:1
DOI 10.1186/s40488-017-0055-6

Journal of Statistical Distributions and Applications

RESEARCH Open Access

Simulation of polyhedral convex contoured distributions

Wolf-Dieter Richter* and Kay Schicker

*Correspondence:
wolf-dieter.richter@uni-rostock.de
Institute of Mathematics, University of Rostock, Ulmenstr. 69, Haus 3, Rostock, 18057, Germany

Abstract

In low dimensions, the relatively easily implementable acceptance-rejection method for generating polyhedral convex contoured uniform distributions is compared to more sophisticated particular methods from the literature, and applied to drug combination studies. Based upon a stochastic representation, the method is extended to the general class of polyhedral convex contoured distributions of known dimension. Based upon a geometric measure representation, an algorithm for simulating corresponding probabilities of rather arbitrary random events is derived.

Keywords: Acceptance-rejection method, Polyhedral convex contoured uniform distribution, Minkowski functional, Geometric and stochastic representation, The class of polyhedral convex contoured distributions, Simulation of distributions and probabilities

Mathematics Subject Classification (2000): MSC 65C05, MSC 62E15, MSC 68U20

1 Introduction

The need of uniform distributions on convex polyhedra appears for various purposes of statistical modeling. In the field of computational visualization of unstructured data, uniform designs on convex polyhedra are used as space filling designs to create three dimensional pictures on the computer, see e.g. (Cutler et al. 2004; Rocchini and Cignoni 2000). The simulation of uniform distributions on convex polyhedra applies in the field of drug combination studies as described in (Fang and Yang 2000; Tan et al. 2003; Tian et al. 2009) which is of special interest in this paper. In (Richter and Schicker 2014) the simulation of a uniform distribution on a tetrahedron is used to detect optimal production schedules.

(Tian et al. 2009) consider a combination study of two drugs with linear dose-response curves. These curves represent the low dose for agents like ionizing radiation, enzyme inhibitions or mutagens. If x_i denotes the dose of drug A_i, $i = 1, 2$ then the single dose-response curves of A_1 and A_2 are assumed to be represented by

$$f_1(x_1) = \alpha_1 + \beta_1 x_1 \text{ and } f_2(x_2) = \alpha_2 + \beta_2 x_2 = \alpha_1 + \beta_2 \left(x_2 - \frac{\alpha_1 - \alpha_2}{\beta_2} \right),$$

where $\alpha_i \in \mathbb{R}$ and $\beta_i \in \mathbb{R}$, $i = 1, 2$ denote regression coefficients. If $x_2^* = x_2 - (\alpha_1 - \alpha_2)/\beta_2$ then the domain for dose ranges of interest is assumed to be

$$\mathbb{P}(a_0, b_0) = \{(x_1, x_2^*)^T \in \mathbb{R} : a_0 \leq \alpha_1 + \beta_1 x_1 + \beta_2 x_2^* \leq b_0, x_1 > 0, x_2^* > 0\} \quad (1)$$

which is an irregular tetragon in $\mathbb{R}^2$. The constants a_0 and b_0 are pre-specified constants, chosen by pharmacological experts. For further details, we refer to (Tian et al. 2009). Since in (Tan et al. 2003) it is proved that a uniform design on $\mathbb{P}(a_0, b_0)$ maximizes the minimum power of the F-test to detect significant deviations from additive actions of the drugs, it is of importance to be able to effectively simulate the uniform distribution on general tetragons $\mathbb{P}(a_0, b_0)$.

In (Tian et al. 2009) several algorithms for the simulation of uniformly distributed random points on convex polyhedra are presented for particular two, three, and n-dimensional cases. The presented algorithms require a pool of analytical as well as probabilistic methods, in dimensions $n > 2$ also numerical methods especially for integration and root computation. They give challenging and individual solutions for the simulation of uniformly distributed random points on special subclasses of convex polyhedra.

In this paper, we present a rather simple but general simulation algorithm using basic geometric-analytical properties of the class of convex polyhedra as well as basic probabilistic simulation methods. This algorithm reduces the mathematical complexity and, since numerical methods for integration and root computation are not necessary, the computational complexity, too. Furthermore, the structure of this algorithm will be the same for every convex polyhedron in $\mathbb{R}^n$ which makes the algorithm flexible to use. Its basic idea is to effectively construct the Minkowski functional of a convex polyhedron and then to apply a fast and simple acceptance-rejection method.

It turns out that this idea simply extends to simulate both distributions from much more general classes of probability distributions and probabilities of rather arbitrary random events measured with respect to any of these distributions. The construction and simulation of multivariate probability distributions and their event probabilities is one of the current challenges in probability theory and statistics. It is possible to characterize a multivariate density by the geometry of its density level sets. For an overview about this broad field of research, we refer to (Arnold et al. 2008; Balkema et al. 2010; Fang et al. 1990; Fernandez and Osiewalski 1995; Gupta and Song 1997; Kamiya et al. 2008; Richter 2009; 2013; 2014; 2015a; 2015b; Richter and Schicker 2017; Sarabia and Gomez-Deniz 2008). Convex polyhedral distributions are characterized by contours being the topological boundaries of convex polyhedra and can be considered being a subclass of polyhedral star-shaped distributions that are studied in (Richter and Schicker 2017). To simulate them needs just the additional independent simulation of a positive random variable playing the role of a certain generalized radius variable of a generalized ball. This way, we widen the flexibility of our approach by describing how arbitrary continuous distributions, having convex polyhedral density level sets, can be constructed and simulated with the new method.

The paper is structured as follows. We describe the main ways of describing convex polyhedra and their Minkowski functionals in Section 2.1 and 2.2, respectively. In Section 3 we present the acceptance-rejection algorithm for generating the uniform distribution on an arbitrary convex polyhedron in $\mathbb{R}^n$. Comparisons of the general acceptance-rejection algorithm with particular algorithms from the literature and applications to drug combination studies are given in Section 4. A general technique from

(Richter 2014, 2015a; Richter and Schicker 2017) is summarized in Section 5.1 to construct the general class of polyhedral convex contoured distributions from the particular polyhedral convex contoured uniform distribution. Sections 5.2 and 5.3 deal with applications of the presented geometric and stochastic representations to simulating probabilities of random events and to linear transformations, respectively. A final discussion including some remarks on the closely related recent paper (Nolan 2016) and several examples are presented in Section 6 and the Appendix, respectively.

2 Representations of convex polyhedra

2.1 $\mathcal{V}$- and $\mathcal{H}$-representations of convex polyhedra

Representations of convex polyhedra are considered in the broad literature of convex geometry, see e.g. (Böhm and Hertel 1980; Ziegler 1995). Here, we recall two standard representations of convex polyhedra that are very fruitful for the purposes in this paper. It is said that a convex polyhedron $\mathbb{P}$, $\mathbb{P} \subset \mathbb{R}^n$, is defined by its vertices $p_1, \ldots, p_l \in \mathbb{R}^n$ if

$$\mathbb{P} = conv(\{p_1, \ldots, p_l\}), \tag{2}$$

where $conv(M)$ denotes the convex hull of the point set M. Alternatively, it is possible to represent $\mathbb{P}$ as the intersection of suitably chosen closed half-spaces. In this case there exist a matrix $A \in \mathbb{R}^{k \times n}$ and a vector $b \in \mathbb{R}^k$ such that

$$\mathbb{P} = \{x \in \mathbb{R}^n : Ax \leq b\}, \tag{3}$$

where "$\leq$" is interpreted componentwise. Note that (2) and (3) are equivalent and there exists software to convert a given representation (2) into a representation (3), and vice versa. In this regard, we refer to (Avis 2000; Fukuda and Prodon 1996). For an illustration of the construction of (2) and (3), see Example 3 in the Appendix.

2.2 Minkowski functionals of convex polyhedra

In case one wants to decide according to an acceptance-rejection algorithm whether a point x from a sample space $\mathbb{R}^n$ belongs to the Euclidean ball of radius r, or not, one can equivalently observe whether the Euclidean norm of x is less or equal to r, $||x|| \leq r$. If B denotes the Euclidean unit ball in $\mathbb{R}^n$, and h_B the Minkowski functional of B defined by $h_B(z) = \inf\{r > 0 : z \in rB\}$, $z \in \mathbb{R}^n$, then $||x|| \leq r$ iff $h_B(x) \leq r$. Imagine B is replaced by a convex polyhedron $\mathbb{P} \in \mathbb{R}^n$ containing the origin as an inner point, $0_n \in int(\mathbb{P})$, where we define $int(\mathbb{P})$ to be the interior of $\mathbb{P}$. It is then possible to specify vector b in representation (3) to be a vector with exclusively positive real entries, i.e. $b \in \mathbb{R}^k_+$. From this, we can conclude that

$$\mathbb{P} = \{x \in \mathbb{R}^n : A'x \leq \mathbb{1}_n\},$$

where $A = (a_{ij})_{i \in \{1,\ldots,k\}, j \in \{1,\ldots,n\}}$ is chosen according to (3), $A' = (A'_1, \ldots, A'_k)^T = (a_{ij}/b_i)_{i \in \{1,\ldots,k\}, j \in \{1,\ldots,n\}}$ and $\mathbb{1}_n$ denotes the n-dimensional vector of ones. Thus

$$\begin{aligned}\mathbb{P} &= \{x \in \mathbb{R}^n : A'_1x \leq 1, A'_2x \leq 1, \ldots, A'_kx \leq 1\} \\ &= \{x \in \mathbb{R}^n : \max\{A'_1x, A'_2x, \ldots, A'_kx\} \leq 1\}.\end{aligned}$$

The last equations show that it is possible to represent a convex polyhedron $\mathbb{P} \subset \mathbb{R}^n$ with the help of the functional $\max\{A_1'x, A_2'x, \ldots, A_k'x\}$ and since

$$\begin{aligned}\inf\{r > 0 : x/r \in \mathbb{P}\} &= \inf\{r > 0 : \max\{A_1'x/r, \ldots, A_k'x/r\} \leq 1\} \\ &= \inf\{r > 0 : \max\{A_1'x, \ldots, A_k'x\} \leq r\} = \max\{A_1'x, \ldots, A_k'x\}, x \in \mathbb{R}^n\end{aligned}$$

we observe that the function

$$h_{\mathbb{P}}(x) = \max\{A_1'x, \ldots, A_k'x\}, x \in \mathbb{R}^n \tag{4}$$

is the Minkowski functional of $\mathbb{P}$. One can represent thus the polyhedron as $\mathbb{P} = \{x \in \mathbb{R}^n : h_{\mathbb{P}}(x) \leq 1\}$. A particular case is dealt with in Example 4 in the Appendix.

3 A general acceptance-rejection simulation algorithm (ARSA)

In this section we introduce an algorithm to simulate uniformly distributed random points on an arbitrarily given multivariate convex polyhedron. To this end, we combine the representations presented in the latter section with the method of acceptance-rejection sampling that was introduced first in (von Neumann 1951). To start with, we assume $\mathbb{P} \subset \mathbb{R}^n$ to be a convex polyhedron, given by representation (3), and choose a cuboid Q containing $\mathbb{P}$, $Q \supseteq \mathbb{P}$. We simulate uniformly distributed random points $x \in Q$ on Q and accept them as uniformly distributed on $\mathbb{P}$, if $x \in \mathbb{P}$, i.e. $Ax \leq b$ according to (3). In Algorithm 1 we summarize the algorithm generating polyhedral convex contoured uniform distributions.

Algorithm 1: Sampling algorithm for uniform distributions on convex polyhedra.

Assumption $\mathbb{P} \subset \mathbb{R}^n$ *is a convex polyhedron, represented by* $\mathbb{P} = \{x \in \mathbb{R}^n : Ax \leq b\}$; $Q \supseteq \mathbb{P}$, *where* $Q = [q_{min,1}, q_{max,1}] \times \ldots \times [q_{min,n}, q_{max,n}]$

Input: A, b, $q_{min,1}, \ldots, q_{min,n}, q_{max,1}, \ldots, q_{max,n}$

Output: $X = (X_1, \ldots, X_n)^T$ uniformly distributed on $\mathbb{P}$

Algorithm

1. Sample uniformly and independent X_1 from $[q_{min,1}, q_{max,1}]$,..., X_n from $[q_{min,n}, q_{max,n}]$ until $A(X_1, \ldots, X_n)^T \leq b$.

Return X

The proofs of that this method stops within a finite time and that the resulting sample points are uniformly distributed on $\mathbb{P}$ can be done analogously to those in Appendix 1 of (Kalke and Richter 2013). A suitable cuboid Q can be found, applying representation (2) of $\mathbb{P}$. One can always find $q_{min,i}$ and $q_{max,i}$, $i = 1, \ldots, n$ by

$$q_{min,i} = \min\{p_j[i], j = 1, \ldots, l\} \text{ and } q_{max,i} = \max\{p_j[i], j = 1, \ldots, l\}, i = 1, \ldots, n,$$

where $p_j[i]$ denotes the ith component of vertex p_j. Applying (3) one can numerically solve for every $i = 1, \ldots, n$ the optimization problems: minimize $q_{min,i} = x_i$ (maximize $q_{max,i} = x_i$), subject to $A(x_1, \ldots, x_n)^T \leq b$.

4 Simulations in particular classes of convex polyhedra

4.1 Uniform distributions in tetragons in $\mathbb{R}^2$

4.1.1 Method of Tian, Fang, Tan, Qin and Tang

In (Tian et al. 2009) a particular algorithm is presented to simulate uniformly distributed random points on an arbitrary two dimensional tetragon that is declared by its vertices a_1, a_2, a_3 and a_4, $\mathbb{P}(a_1, a_2, a_3, a_4) \subset \mathbb{R}^2$. It is shown there that a uniformly on $\mathbb{P}(a_1, a_2, a_3, a_4)$ distributed random vector X allows the stochastic representation

$$X \stackrel{d}{=} (a_1, a_2, a_3, a_4) \begin{pmatrix} (1 - Y_1)(1 - Y_2) \\ Y - 1(1 - Y_2) \\ Y_1 Y_2 \\ (1 - Y_1) Y_2 \end{pmatrix},$$

where the random vector $Y = (Y_1, Y_2)^T$ follows the density function $f_Y(y_1, y_2) = \frac{d_0 + d_1 y_1 + d_2 y_2}{d_0 + 0.5(d_1 + d_2)}$ with $d_0 = |a_2 - a_1, a_4 - a_1|$, $d_1 = |a_2 - a_1, a_3 - a_4|$ and $d_2 = |a_3 - a_2, a_4 - a_1|$ where $|.,.|$ denotes a determinant. The simulation of Y is realized, applying the inverse transform sampling of the marginal distributions of Y that can be found in (Tian et al. 2009).

4.1.2 The alternative method: **ARSA**

Our general acceptance-rejection simulation Algorithm 1 presented in Section 3 offers an alternative method to that of the latter section and applies immediately. One has only to calculate the matrix A and the vector b from the given vertices $a_1, \ldots, a_4$ such that (3) holds. To this, it is possible to apply the algorithms described in (Fukuda and Prodon 1996; Avis 2000). In the following, however, we present an alternative method that uses only elementary theory from linear algebra. To this end, let the points $a_i = (x_i, y_i)^T$, $i = 1, \ldots, 4$, be ordered anticlockwise and let $(x, g_{a_i,a_j}(x))^T$ denote a point from the line through the points a_i and a_j, $j = i + 1$ if $i = 1, 2, 3$ and $j = 1$ if $i = 4$. Then,

$$\frac{g_{a_i a_j}(x) - y_i}{y_j - y_i} = \frac{x - x_i}{x_j - x_i}$$

is equivalent to

$$(y_j - y_i)x - (x_j - x_i) g_{a_i a_j}(x) = x_i y_j - x_j y_i,$$

where $(y_j - y_i, -(x_j - x_i))^T$ denotes the outer normal vector of the line through the points a_i and a_j. With $m_{i,j} = x_i y_j - x_j y_i$, $i, j \in \{1, \ldots, 4\}$, $i \neq j$,

$$A = \begin{pmatrix} y_2 - y_1 & -(x_2 - x_1) \\ y_3 - y_2 & -(x_3 - x_2) \\ y_4 - y_3 & -(x_4 - x_3) \\ y_1 - y_4 & -(x_1 - x_4) \end{pmatrix} \text{ and } b = \begin{pmatrix} m_{1,2} \\ m_{2,3} \\ m_{3,4} \\ m_{4,1} \end{pmatrix},$$

one gets the representation $\mathbb{P}(a_1, a_2, a_3, a_4) = \{(x, y)^T \in \mathbb{R}^2 : A(x, y)^T \leq b\}$. A particular numerical situation and a more general application to the drug combination study are considered in Examples 5 and 6, respectively, in the Appendix.

4.2 Uniform distributions in triangular prisms in $\mathbb{R}^3$

4.2.1 Method of Tian, Fang, Tan, Qin and Tang

Apart from the simulation of uniform distributions on tetragons in (Tian et al. 2009), the presented method is transferred there to the class of triangular prisms in $\mathbb{R}^3$. A

triangular prism $\mathbb{P}(a_1, a_2, a_3, a_4, a_5, a_6)$ is defined by its six vertices a_1, a_2, a_3, a_4, a_5 and $a_6 \in \mathbb{R}^3$, where $conv(\{a_1, a_2, a_3\})$ and $conv(\{a_4, a_5, a_6\})$ each forms a triangular base of $\mathbb{P}(a_1, \ldots, a_6)$ and $\overline{a_1a_4}$, $\overline{a_2a_5}$ and $\overline{a_3a_6}$ each forms an edge of $\mathbb{P}(a_1, \ldots, a_6)$. It is shown in (Tian et al. 2009) that a uniformly on $\mathbb{P}(a_1, \ldots, a_6)$ distributed random vector X allows the stochastic representation

$$X \overset{d}{=} (a_1, a_2, a_3, a_4, a_5, a_6) \begin{pmatrix} (1 - Y_1 - Y_2)(1 - Y_3) \\ Y_1(1 - Y_3) \\ Y_2(1 - Y_3) \\ (1 - Y_1 - Y_2)Y_3 \\ Y_1Y_2 \\ Y_2Y_3 \end{pmatrix},$$

where $Y = (Y_1, Y_2, Y_3)^T$ follows the density $f_Y(y_1, y_2, y_3)$ given by (3.2)-(3.6) in (Tian et al. 2009). By deriving marginal and conditional densities of f_Y a conditional sampling for Y is presented there using numerical methods.

4.2.2 **ARSA** *for triangular prisms in* $\mathbb{R}^3$

As in the previous section, it is again possible to apply our general Algorithm 1 by calculating the matrix A, the vector b and a cuboid Q for triangular prisms. This can be done computationally as described in Section 2.1 or by adopting the **ARSA** similarly as we did already for the simulation of uniform distributions on tetragons in Section 4.1.2.

Given the vertices $a_j = (a_{j1}, a_{j2}, a_{j3})$, $j = 1, \ldots, 6$ of the triangular prisma $\mathbb{S}(a_1, \ldots, a_6)$, one can represent the planes of which $conv(\{a_1, a_2, a_3\})$, $conv(\{a_1, a_2, a_4, a_5\})$, $conv(\{a_2, a_3, a_5, a_6\})$, $conv(\{a_1, a_3, a_4, a_6\})$ and $conv(\{a_4, a_5, a_6\})$ are subsets as $\{(x, y, z)^T \in \mathbb{R}^3 : n_i \cdot (x, y, z)^T = \lambda_i\}$, $i = 1, \ldots, 5$, respectively, where

$$\begin{aligned} &n_1 = (a_2 - a_1) \times (a_3 - a_1),\ \lambda_1 = n_1a_1,\ n_2 = (a_2 - a_1) \times (a_4 - a_1),\ \lambda_2 = n_2a_1, \\ &n_3 = (a_5 - a_2) \times (a_3 - a_2),\ \lambda_3 = n_3a_2,\ n_4 = (a_1 - a_3) \times (a_6 - a_3),\ \lambda_4 = n_4a_3, \\ &n_5 = (a_5 - a_4) \times (a_6 - a_4),\ \lambda_5 = n_5a_4, \end{aligned}$$

the symbol "$\times$" denotes the vector cross product, n_i is a normal vector of the considered plane and λ_i is the Euclidean distance of the plane from the origin, $i = 1, \ldots, 5$. With $A' = (n_1, n_2, n_3, n_4, n_5)^T$ and $b' = (\lambda_1, \lambda_2, \lambda_3, \lambda_4, \lambda_5)^T$ one gets the representation $\mathbb{P}(a_1, \ldots, a_6) = \{(x, y, z)^T \in \mathbb{R}^3 : A(x, y, z)^T \leq b\}$ by considering $A'a_i$ for every $i = 1, \ldots, 6$ and comparing $A'a_i$ with b' componentwise. If a component of $A'a_i$ is greater than the component of b', one multiplies the considered row of A' and the component of b' by -1 and continues with the next edge and the transformed A' and b'. This method results in matrix A and vector b and thus the desired representation of $\mathbb{P}(a_1, \ldots, a_6)$, and is summarized by Algorithm 2. A suitable cuboid Q can be chosen as

$$\begin{aligned} Q = &[\min\{a_{11}, \ldots, a_{61}\}, \max\{a_{11}, \ldots, a_{61}\}] \times \\ &[\min\{a_{12}, \ldots, a_{62}\}, \max\{a_{12}, \ldots, a_{62}\}] \times [\min\{a_{13}, \ldots, a_{63}\}, \max\{a_{13}, \ldots, a_{63}\}]. \end{aligned}$$

For a particular numerical illustration and a more general application to the drug combination study, see Examples 7 and 8, respectively, in the Appendix.

Algorithm 2: Calculate representation (3) of $\mathbb{P}(a_1,\ldots,a_6)$ from $\mathbb{S}(a_1,\ldots,a_6)$.

Input: A', b', a_1, a_2, a_3, a_4, a_5, a_6

Output: A, b

Algorithm

$A_0 := A'$; $b_0 := b'$;
for $i := 1$ to 6 step 1 **do**
  $z_i := A_{i-1}a_i$;
  for $j := 1$ to 5 step 1 **do**
    if $z_i[j] > b_{i-1}[j]$ **then**
      $A_{i-1}[j,] := (-1)\cdot A_{i-1}[j,]$;
      $b_{i-1}[j] := (-1)\cdot b_{i-1}[j]$;
    end if
  end for
  $A_i := A_{i-1}$; $b_i := b_{i-1}$;
end for

Return $A := A_6$, $b := b_6$

5 Polyhedral convex contoured distributions

In this section we are going beyond uniformity and show a flexible method to construct arbitrary continuous distributions having convex polyhedra as density level sets, which we call polyhedral convex contoured distributions. Our starting point is the consideration of the uniform distribution on a convex polyhedron in the latter sections. In Section 5.1 we summarize certain stochastic and geometric representations and linear transformation methods from (Richter 2014; 2015a) and (Richter and Schicker 2017) for the particular classes of convex polyhedra and polyhedral convex contoured distributions, respectively. Specific applications of representations (6) and (4) below are presented in Sections 5.2 and 5.3, respectively.

5.1 Geometric and stochastic representations

Since the class of convex polyhedra is both a subclass of the class of star bodies and a subclass of convex bodies, we can apply the stochastic and geometric representations from these cases, to construct polyhedral convex contoured distributed random vectors. To this end, let $\mathbb{P} \subset \mathbb{R}^n$ be a convex polyhedron having the origin 0_n in its interior, i.e. $0_n \in int(\mathbb{P})$. Let $G = (G_1,\ldots,G_n)^T$ be a random vector uniformly distributed on $\mathbb{P}$, then the random vector $U = G/h_{\mathbb{P}}(G)$ is generalized uniformly distributed on the topological boundary $\mathbb{S} = \{x \in \mathbb{R}^n : h_{\mathbb{P}}(x) = 1\}$ of $\mathbb{P}$, $U \sim \omega_{\mathbb{S}}$. The probability measure $\omega_{\mathbb{S}}$ is defined for every Borel measurable set $A \in (\mathfrak{B}^n \cap \mathbb{S})$ by $\omega_{\mathbb{S}}(A) = \mathfrak{O}_{\mathbb{S}}(A)/\mathfrak{O}_{\mathbb{S}}(\mathbb{S})$, where $\mathfrak{O}_{\mathbb{S}}$ is called the star-generalized surface measure according to (Richter 2014). It is defined considering the central projection cone $CPC(A) = \{x \in \mathbb{R}^n : x/h_{\mathbb{P}}(x) \in A\}$ and the star sector of radius $\rho > 0$, $sector(A,\rho) = CPC(A) \cap [\,\rho\mathbb{P}]$ for every $A \in (\mathfrak{B}^n \cap \mathbb{S})$, by

$$\mathfrak{O}_{\mathbb{S}}(A) = f'(1), \text{where } f(\rho) = \mu(sector(A,\rho)), A \in (\mathfrak{B}^n \cap \mathbb{S}).$$

While this definition deals with taking derivatives of volumes of suitably chosen sectors of convex polyhedra, it is also possible to introduce an equivalent way of defining $\mathfrak{O}_{\mathbb{S}}$ using integration and replacing the Euclidean norm of the vector normal to the sphere in

the defining integral of the Euclidean surface content by a suitably chosen non-Euclidean norm. If $h_{\mathbb{P}}$ denotes a norm and $N(\vartheta) = (\nabla\eta(\vartheta), -1)^T$ is the outer normal vector to the norm sphere $\mathbb{S}$ at the point $(\vartheta^T, \eta(\vartheta))^T$, then, with notations as in (4), $\mathfrak{O}_{\mathbb{S}}$ satisfies the dual norm representation

$$\mathfrak{O}_{\mathbb{S}}(A) = \int\limits_{G(A)} \max\{p_1^T N(\vartheta), \ldots, p_l^T N(\vartheta)\} d\vartheta,\ A \in (\mathfrak{B}^n \cap \mathbb{S})^+, \tag{5}$$

where $G(A) = \{\vartheta \in \mathbb{R}^{n-1} : \exists\eta = \eta(\vartheta) \text{with } (\vartheta^T, \eta)^T \in A\}$ and $(\mathfrak{B}^n \cap \mathbb{S})^+$ denotes the Borel σ-field on the upper half-sphere of $\mathbb{S}$. For the proof of (5) and further integral representations of the star-generalized surface measure of star-shaped polyhedra, we refer to (Richter and Schicker 2017).

Let us recall that since $0_n \in int(\mathbb{P})$ it is possible to calculate the Minkowski functional $h_{\mathbb{P}}$ of $\mathbb{P}$ as described in Section 2.2.

Let $g : \mathbb{R}_+ \to \mathbb{R}_+$ satisfy the assumptions $0 < \mathcal{I}(g) < \infty$ where $\mathcal{I}(g) = \int\limits_0^\infty r^{n-1} g(r) dr$. We call g a density generating function (*dgf*) and a random vector X taking values in $\mathbb{R}^n$ polyhedral convex contoured distributed, if X allows the stochastic representation

$$X \stackrel{d}{=} R_g \cdot U, \tag{6}$$

where R_g and U are stochastically independent, $U \sim \omega_{\mathbb{S}}$ and R_g follows the density $f(r) = \frac{1}{\mathcal{I}(g)} r^{n-1} g(r)$, $r > 0$. Note that the density of X can be represented as

$$\varphi_{g,\mathbb{P}}(x) = C(g, \mathbb{P}) g(h_{\mathbb{P}}(x)), x \in \mathbb{R}^n, \tag{7}$$

where $C(g, \mathbb{P}) = 1/(n\mu(\mathbb{P})\mathcal{I}(g))$ is a normalizing constant and μ denotes the Lebesgue measure in $\mathbb{R}^n$. The probability measure having the density $\varphi_{g,\mathbb{P}}$ will be denoted by $\Phi_{g,\mathbb{P}}$ and $\mathbb{P}$ will be called the contour defining polyhedral convex body or the contour defining convex polyhedron. We recall the geometric measure representation formula of $\Phi_{g,K}(B)$ for every $B \in \mathfrak{B}^n$,

$$\Phi_{g,\mathbb{P}}(B) = C(g, \mathbb{P}) \int\limits_0^\infty r^{n-1} g(r) \mathfrak{O}_{\mathbb{S}} \left(\left[\frac{1}{r} B \right] \cap \mathbb{S} \right) dr = \frac{1}{\mathcal{I}(g)} \int\limits_0^\infty r^{n-1} g(r) \mathfrak{F}_{\mathbb{S}}(B, r) dr \tag{8}$$

where $r \to \mathfrak{F}_{\mathbb{S}}(B, r) = \omega_{\mathbb{S}} \left(\left[\frac{1}{r} B \right] \cap \mathbb{S} \right)$ denotes the star intersection-proportion function (ipf) of the set B. Note that if $\mathfrak{O}_{\mathbb{S}}$ satisfies the dual norm representation (5) it holds

$$\Phi_{g,\mathbb{P}}(B) = C(g, \mathbb{P}) \int\limits_0^\infty \int\limits_{G\left(\left[\frac{1}{r} B\right] \cap \mathbb{S}\right)} r^{n-1} g(r) \max \left\{ p_1^T N(\vartheta), \ldots, p_l^T N(\vartheta) \right\} d\,\vartheta\, dr.$$

For further specific geometric representation formulae of polyhedral star-shaped distributions, having star-shaped polyhedra as contour defining polyhedron, see again (Richter and Schicker 2017).

For the choice of a *dgf* g there are various possibilities. For some basic types of density generating functions, we refer to (Fang et al. 1990; Richter and Schicker 2017). Note that if we choose $g(r) = I_{(0,1]}(r)$, where $I_{(0,1]}$ is the indicator function on the interval $(0, 1]$, we get the uniform distribution on $\mathbb{P}$.

Finally, we want to show that in certain situations it is possible to find exact representations of $\mathfrak{F}_{\mathbb{S}}(B, r)$ in Eq. (8). If we consider $\Phi_{g,\mathbb{P}}(B(\rho))$, where $B(\rho) = \rho\mathbb{P}$, $\rho > 0$, then $\mathfrak{F}_{\mathbb{S}}(B(\rho), r) = I_{[0,\rho)}(r)$, $r > 0$, and

$$\Phi_{g,\mathbb{P}}(B(\rho)) = \frac{1}{\mathcal{I}(g)} \int_0^\rho r^{n-1} g(r) dr.$$

Let us consider R_g^2, then

$$\frac{d}{dy} P(R_g^2 < y) = \frac{d}{dy} \Phi_{g,\mathbb{P}}(B(\sqrt{y})) = \frac{y^{n/2-1} g(\sqrt{y})}{2\mathcal{I}(g)}, y > 0.$$

In slightly modified notation, this function is known from (Richter 1991) as the density of the g-generalized χ^2-distribution with n degrees of freedom.

5.2 Simulating probabilities $\Phi_{g,\mathbb{P}}(B)$

In this section we use the geometric measure representation formula (8) of multivariate polyhedral convex contoured probability distributions for simulating single values of this distribution by simulating the corresponding *dgf* g and the generalized uniform distribution $\omega_{\mathbb{S}}$. Given a *dgf* g, a contour defining convex polyhedron $\mathbb{P} \subset \mathbb{R}^n$ and a set $B \subseteq \mathfrak{B}^n$ we can approximate $\Phi_{g,\mathbb{P}}(B)$ with the following method. Choose an integer $k \in \mathbb{N}$, simulate k uniformly on $\mathbb{P}$ distributed points $X_{(j)}$, $j = 1, \ldots, k$ using Algorithm 1. For every $j = 1, \ldots, k$ generate generalized uniformly on $\mathbb{S}$ distributed random points $Y_{(j)}$ by $Y_{(j)} = X_{(j)}/h_{\mathbb{P}}(X_{(j)})$. Now, choose $u \in \mathbb{R}^+$ as upper boundary of the integration interval of $r \in (0, u]$ and an increment $1/v$, $v \in \mathbb{N}^+$. For every t, $t = 0, 1, \ldots, uv$ consider $t/v \cdot Y_{(j)}$, $j = 1, \ldots, k$, count how often $(t/v \cdot Y_{(j)}) \in B$ and store the number in $p(t/v)$,

$$p(t/v) = \#\left\{ j \in \{1, \ldots, k\} : \frac{t}{v} Y_{(j)} \in B \right\},$$

where # means "number of cases". Now approximate $\mathfrak{F}_{\mathbb{S}}(B, t/v)$ by $p(t/v)/k$ and calculate

$$integrand(t/v) = (t/v)^{n-1} \cdot g(t/v) \cdot p(t/v)/k.$$

$\Phi_{g,\mathbb{P}}(B)$ is now approximated by numerical integration of $integrand(t/v)$ from 0 to u using the mesh points t/v, $t = 0, 1, \ldots, uv$. For the numerical integration use common rules like e.g. Simpson's integration rule. This method is summarized in Algorithm 3.

Example 1

We consider the symmetric octagon having the vertices $p_1 = (1, 0)^T$, $p_2 = (3/4, 3/4)^T$, $p_3 = (0, 1)^T$, $p_4 = (-3/4, 3/4)^T$, $p_5 = (-1, 0)^T$, $p_6 = (-3/4, -3/4)^T$, $p_7 = (0, -1)^T$ and $p_8 = (3/4, -3/4)^T$ as contour defining convex polyhedron $\mathbb{P}$. In (Richter and Schicker 2017) it is shown that

$$h_{\mathbb{P}}(x, y) = \max\{|x|, |y|\} + \frac{1}{3} \min\{|x|, |y|\}, (x, y)^T \in \mathbb{R}^2.$$

We choose the multinormal-type density generator $g(r) = e^{-r^2/2}$ and consider the polyhedral convex contoured density

$$\varphi_{g,\mathbb{P}}(x, y) = \frac{1}{6} e^{-\frac{1}{2}(\max\{|x|,|y|\} + \frac{1}{3}\min\{|x|,|y|\})^2}, (x, y)^T \in \mathbb{R}^2.$$

For a particular illustration of $\varphi_{g,\mathbb{P}}$ and a simulation of a sample point cloud of the corresponding distribution $\Phi_{g,\mathbb{P}}$, we refer to Fig. 1.

For a concrete application of Algorithm 3 we consider now the set $B = \{(x, y)^T \in \mathbb{R}^2 : x, y \geq 0\}$ and calculate $\Phi_{g,\mathbb{P}}(B)$. Because of the symmetry of $\mathbb{P}$, we can conclude in this case that $\Phi_{g,\mathbb{P}}(B) = 0.25$. Applying Algorithm 3, we choose $v = 100$ and approximate $\Phi_{g,\mathbb{P}}(B)$ with different values of k, $k \in \{10^3, 10^4, 10^5\}$. Since R_g from (6) follows the density $f(r) =$

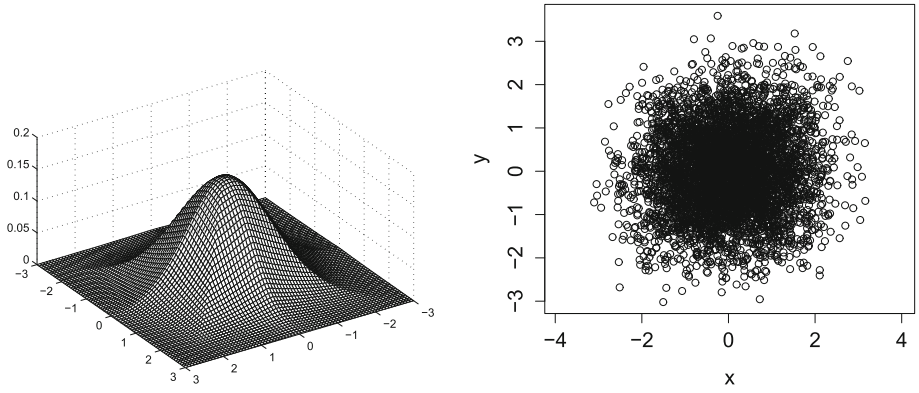

Fig. 1 Density $\varphi_{g,\mathbb{P}}$ (*left*) and a simulated cloud of 5000 points of the distribution $\Phi_{g,\mathbb{P}}$ (*right*)

$re^{-r^2/2}$ and the 99.999 percent quantile of the distribution of R_g is 4.7985, we choose $u = 5$. As numerical integration method we use the Simpson rule in Algorithm 3. Note that it is also possible to apply *integrand* from Algorithm 3 for adaptive numerical integration rules that calculate the mesh points more flexibly than static numerical integration rules. For a comparison we used the adaptive Simpson quadrature, the Gauss-Kronrod quadrature

Algorithm 3: Simulation of $\Phi_{g,\mathbb{P}}(B)$.

Input: g, $\mathbb{P}$, $h_{\mathbb{P}}$ B, k, u, v
Output: $\Phi_{g,\mathbb{P}}(B)$

Algorithm
Initializing *r and integrand are both vectors of length* $u*v+1$
  for $j := 1$ to k step 1 **do**
    Simulate $X_{(j)}$ with Algorithm 1;
  end for
  for $j := 1$ to k step 1 **do**
    $Y_{(j)} = X_{(j)}/h_{\mathbb{P}}(X_{(j)})$;
  end for
  $count := 1$;
  for $i := 0$ to u step $1/v$ **do**
    $p := 0$;
    for $j := 1$ to k step 1 **do**
      if $i \cdot Y_{(j)} \in B$ **then**
        $p := p + 1$;
      end if;
    end for
    $r[count] := i$;
    $integrand\,[count] := i^{n-1} \cdot g(i) \cdot p/k$;
    $count := count + 1$;
  end for
  Calculate $\Phi_{g,\mathbb{P}}(B)$ using numerical integration of *integrand* with vector of mesh points r;

Return $\Phi_{g,\mathbb{P}}(B)$

and the adaptive Lobatto quadrature. These standard routines are available for example in *MATLAB* or in the package *pracma* of the statistic package *R*. The numerical results are shown in Table 1.

5.3 Linear transformations

For another application of the construction method from Section 5.1 it is assumed that the contour defining convex polyhedron $\mathbb{P}$ contains 0_n in its interior. In this section, we will show how to apply this method for arbitrarily chosen convex polyhedra. Let $\mathbb{P} \subset \mathbb{R}^n$ be an arbitrary convex polyhedron in the n-dimensional space and let $c \in int(\mathbb{P})$ be an arbitrary element of the interior of $\mathbb{P}$. The shifted set $\mathbb{P} - c$ will be denoted by $\mathbb{P}_c$, thus $0_n \in int(\mathbb{P}_c)$. Applying now Section 2.2, we can determine $h_{\mathbb{P}_c}$ and can stochastically represent a random vector X_c by applying (6). It follows

$$X_c \stackrel{d}{=} R_g \cdot U_c, \text{where } U_c \sim \omega_{\mathbb{S}_c}$$

and $\mathbb{S}_c$ is the boundary of $\mathbb{P}_c$. Furthermore, the density of X_c is

$$\varphi_{g,\mathbb{P}_c}(x) = C(g, \mathbb{P}_c) g(h_{\mathbb{P}_c}(x)), x \in \mathbb{R}^n.$$

The class of convex polyhedral distributions $\Phi_{g,\mathbb{P}_c}$ is a subclass of the class of polyhedral star-shaped distributions that is considered in (Richter and Schicker 2017). Specific properties, simulation methods as well as examples of application of convex polyhedral distributions are studied in the current article. According to (Richter and Schicker 2017) we can transform X_c linearly to construct a convex polyhedral distributed random vector Y that follows a density with density level sets being located where we chose the contour defining convex polyhedron $\mathbb{P}$. Doing this, it is proven in Theorem 7.1 of (Richter and Schicker 2017) that $Y \stackrel{d}{=} X_c + c$ satisfies the desired properties and follows the density

$$\varphi_{g,\mathbb{P}_c+c}(y) = C(g, \mathbb{P}_c) g(h_{\mathbb{P}_c}(y - c)), y \in \mathbb{R}^n.$$

Example 2 We consider the trapezoid $\mathbb{P}$ having vertices $p_1 = (4,4)^T$, $p_2 = (7,4)^T$, $p_3 = (6,6)^T$ and $p_4 = (5,6)^T$ as contour defining convex polygon, and choose $c = (5,5)^T$ to shift $\mathbb{P}$ by c, see Fig. 2.

Now, $\mathbb{P}_c$ can be represented by (3) as

$$\mathbb{P}_c = \left\{ \begin{pmatrix} x \\ y \end{pmatrix} \in \mathbb{R}^2 : \begin{pmatrix} 0 & -3 \\ 2 & 1 \\ 0 & 1 \\ -2 & 1 \end{pmatrix} \begin{pmatrix} x \\ y \end{pmatrix} \leq \begin{pmatrix} 3 \\ 3 \\ 1 \\ 1 \end{pmatrix} \right\}$$

and thus, according to Section 2.2,

$$h_{\mathbb{P}_c}(x, y) = \max\{-y, 2/3x + y/3, y, -2x + y\}, (x, y)^T \in \mathbb{R}^2.$$

Table 1 Numerical evaluations of $\Phi_{g,\mathbb{P}}(B)$

Method	k:	10^3	10^4	10^5
Simpson rule		0.2359971	0.247997	0.249377
Adaptive Simpson rule		0.2359991	0.2479991	0.2493791
Gauss-Kronrod quadrature		0.2359991	0.2479991	0.2493791
Adaptive Lobatto quadrature		0.2359993	0.2479992	0.2493792

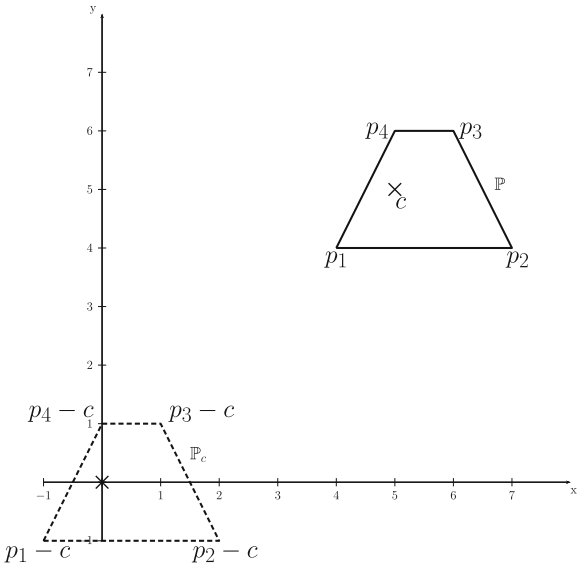

Fig. 2 Contour defining trapezoid $\mathbb{P}$ and the shifted set $\mathbb{P}_c$ from Example 2

Hence,

$$\varphi_{g,\mathbb{P}_c}(x,y) = \frac{1}{8\mathcal{I}(g)} g(\max\{-y, 2/3x + y/3, y, -2x + y\}), (x,y)^T \in \mathbb{R}^2$$

and

$$\varphi_{g,\mathbb{P}_c+c}(x,y) = \frac{1}{8\mathcal{I}(g)} g(\max\{-(y-c), 2/3(x-c) + (y-c)/3, y-c, \\ -2(x-c) + (y-c)\}), (x,y)^T \in \mathbb{R}^2.$$

If we choose, e.g., the density generating function of the uniform distribution, $g_1(r) = I_{[0,1]}(r)$, then $\mathcal{I}(g_1) = 1/2$,

$$\varphi_{g_1,\mathbb{P}_c}(x,y) = \frac{1}{4} I_{[0,1]}(\max\{-y, 2/3x + y/3, y, -2x + y\}), (x,y)^T \in \mathbb{R}^2$$

and

$$\varphi_{g_1,\mathbb{P}_c+c}(x,y) = \frac{1}{4} I_{[0,1]}(\max\{-(y-c), 2/3(x-c) + (y-c)/3, y-c, \\ -2(x-c) + (y-c)\}), (x,y)^T \in \mathbb{R}^2.$$

If we choose alternatively the Kotz-type *dgf* $g_2(r) = r^{18}e^{-20r^2}$, then $\mathcal{I}(g_2) = \Gamma(10)/(2 \cdot 20^{10})$,

$$\varphi_{g_2,\mathbb{P}_c}(x,y) = \frac{20^{10}}{4\Gamma(10)} (h_{\mathbb{P}_c}(x,y))^{18} e^{-20(h_{\mathbb{P}_c}(x,y))^2}, (x,y)^T \in \mathbb{R}^2$$

and

$$\varphi_{g_2,\mathbb{P}_c+c}(x,y) = \frac{20^{10}}{4\Gamma(10)} (h_{\mathbb{P}_c}(x-c, y-c))^{18} e^{-20(h_{\mathbb{P}_c}(x-c,y-c))^2}, (x,y)^T \in \mathbb{R}^2.$$

For an illustration of $\varphi_{g_1,\mathbb{P}_c}$, $\varphi_{g_1,\mathbb{P}_c+c}$, $\varphi_{g_2,\mathbb{P}_c}$ and $\varphi_{g_2,\mathbb{P}_c+c}$, see Figs. 3, 4 and 5.

6 Discussion

(Tian et al. 2009) presented a method for simulating uniform distributions on polyhedral regions which always needs challenging case sensitive representations when it is applied

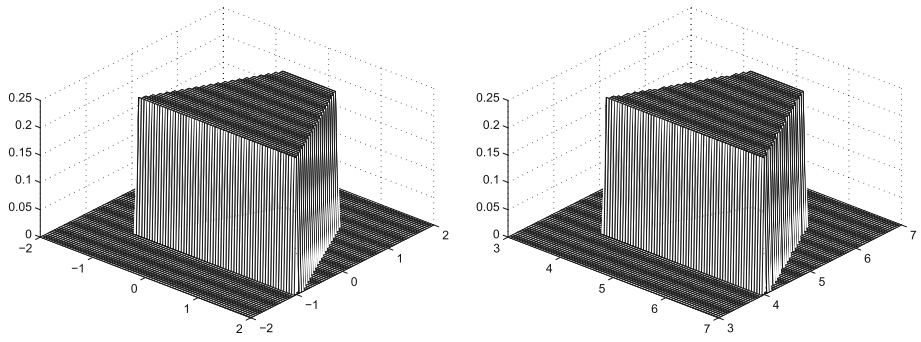

Fig. 3 $\varphi_{g_1,\mathbb{P}_c}$ (*left*) and $\varphi_{g_1,\mathbb{P}_c+c}$ (*right*) from Example 2

to drug combination study. These preparations include the derivation of sophisticated stochastic representations of the uniformly distributed random vectors as presented in Sections 4.1.1 and 4.2.1 as well as non-trivial distributional considerations for the representing random variables sketched also there. Here we establish an alternative approach based upon an acceptance-rejection algorithm which may relatively easily and flexibly be adopted to rather different situations. It will also allow to consider in the future dose-response curves and domains for dose ranges different from that introduced according to (Tian et al. 2009) in Section 1. Moreover, our method allows simulating general polyhedral convex contoured distributions $\Phi_{g,\mathbb{P}}$ and any particular probability $\Phi_{g,\mathbb{P}}(B)$ where the density generating function g allows modeling both heavy and light distribution tails and centers and $\mathbb{P}$ is an arbitrary convex polyhedron. Note, however, that if the probability $\Phi_{g,\mathbb{P}}(B)$ is small which is, e.g., the case if B is a "thin" set or has large distance from the center of the distribution $\Phi_{g,\mathbb{P}}$ then relatively large sample sizes are needed for good approximations via simulation. In such and related cases it may be a useful alternative to try a direct numerical approximation of $\Phi_{g,\mathbb{P}}(B)$ using the geometric measure representation (8) as indicated in Example 1. Fields of successful applications of this type are surveyed, e.g., in (Richter 2014; 2015a; 2015b). The reader is encouraged to find other applications.

Now that the reader has become familiar with the role the stochastic and geometric representations (6) and (8) may play in simulation it is about time to shortly compare

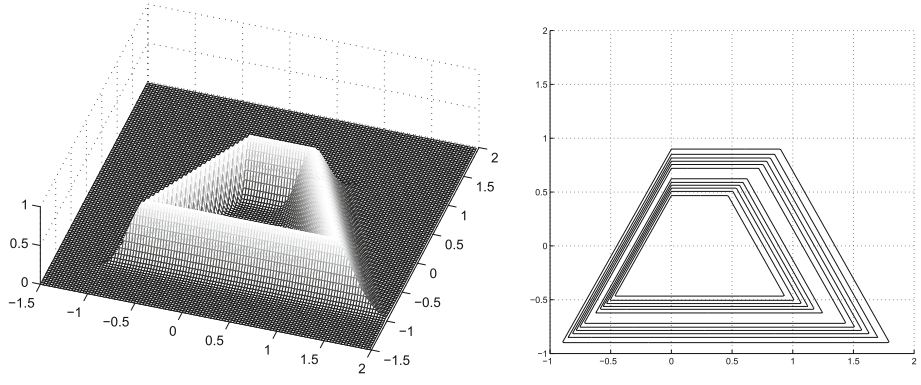

Fig. 4 $\varphi_{g_2,\mathbb{P}_c}$ (*left*), and its density level sets (*right*) from Example 2

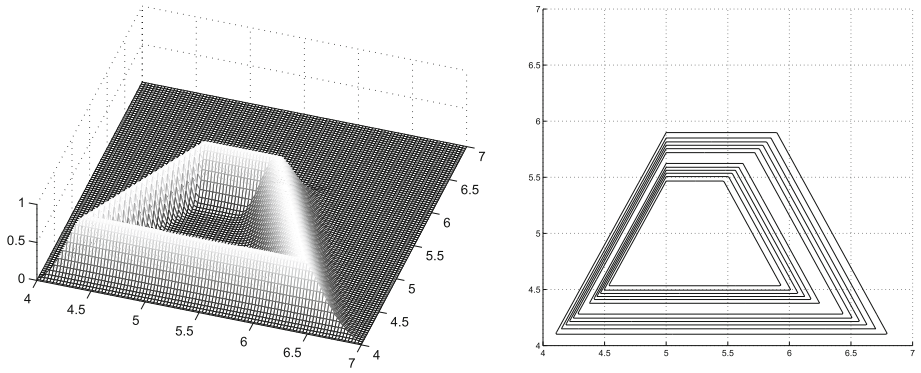

Fig. 5 $\varphi_{g_2,\mathbb{P}_c+c}$ (*left*), and its density level sets (*right*) from Example 2

the approaches presented here and in (Nolan 2016) with each other. The latter one also refers to a stochastic representation like (6) and exploits it in three particular cases for exact simulation. Note that probability models were studied for these particular cases to a certain extent already in (Henschel and Richter 2002) and Richter (2009). In other cases, the stochastic representation is taken in (Nolan 2016) to motivate an approximative simulation method. It would be an interesting aspect of future work to study the resulting approximation accuracy in this approach.

From a purely descriptive point of view, i.e. if we are just given data, visualized by clouds of points, the methods presented here and in (Nolan 2016) may be considered to be attractive alternatives for modeling polyhedral contoured data clouds. But notice that the approach in (Nolan 2016) allows for approximative consideration of much more generalized spherical and related distributions, assuming however an explicit representation of their gauge function is given. It is another aspect of future work to develop exact simulation methods for broader distribution classes.

Appendix

Example 3 Consider triangle $\mathbb{P}$ in Fig. 6. Since $\mathbb{P}$ has vertices $p_1 = (1,-2), p_2 = (2,1)$ and $p_3 = (-2,2)$, it can be represented according to (2) as $\mathbb{P} = conv(\{p_1,p_2,p_3\})$. Choosing the closed half-spaces $H_1 = \{(x,y) \in \mathbb{R}^2 : 3x-y \le 5\}, H_2 = \{(x,y) \in \mathbb{R}^2 : x+4y \le 6\}$ and $H_3 = \{(x,y) \in \mathbb{R}^2 : -4x-3y \le 2\}$, triangle $\mathbb{P}$ can be equivalently represented according to (3) as intersection of these half-spaces,

$$\mathbb{P} = \left\{ \begin{pmatrix} x \\ y \end{pmatrix} \in \mathbb{R}^2 : \underbrace{\begin{pmatrix} 3 & -1 \\ 1 & 4 \\ -4 & -3 \end{pmatrix}}_{=A} \begin{pmatrix} x \\ y \end{pmatrix} \le \underbrace{\begin{pmatrix} 5 \\ 6 \\ 2 \end{pmatrix}}_{=b} \right\}.$$

Example 4 This example is a continuation of the previous one. We consider again triangle $\mathbb{P}$ in Fig. 6. Using representation (3) of $\mathbb{P}$ from Example 3, it follows

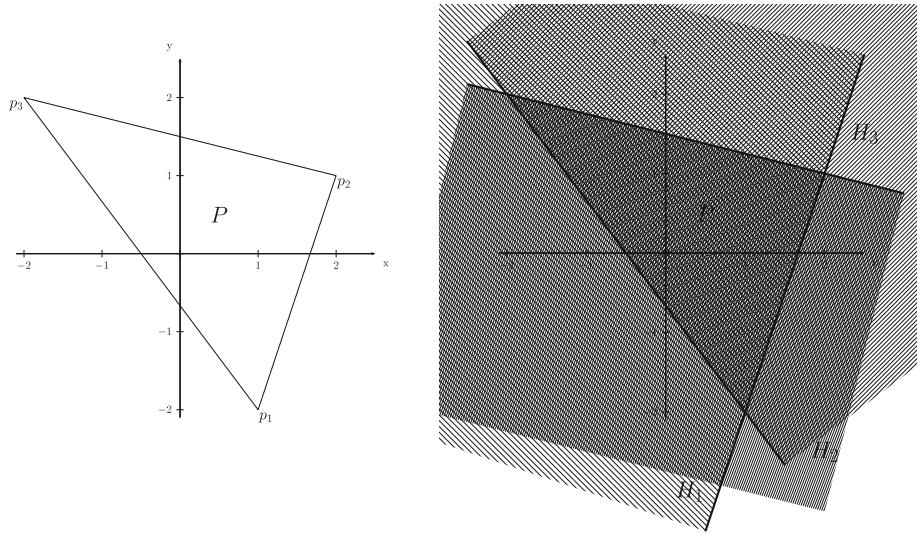

Fig. 6 Triangle $\mathbb{P}$ defined by its vertices (*left*) and by suitably chosen closed half-spaces (*right*)

$A_1' = (3/5, -1/5), A_2' = (1/6, 2/3), A_3' = (-2, -3/2)$, and according to (4) the Minkowski functional $h_{\mathbb{P}}$ can be represented as

$$h_{\mathbb{P}}(x, y) = \max\{3/5x - 1/5y, 1/6x + 2/3y, -2x - 3/2y\}, (x, y)^T \in \mathbb{R}^2.$$

Example 5 Here we illustrate our consideration in Section 4.1.2. To this end, let $\mathbb{P}(a_1, a_2, a_3, a_4)$ be the square with vertices $a_1 = (1, 1)^T$, $a_2 = (2, 1)^T$, $a_3 = (2, 2)^T$ and $a_4 = (1, 2)^T$. Then

$$A = \begin{pmatrix} 0 & -1 \\ 1 & 0 \\ 0 & 1 \\ -1 & 0 \end{pmatrix} \text{ and } b = \begin{pmatrix} -1 \\ 2 \\ 2 \\ -1 \end{pmatrix}.$$

Example 6 Here we apply **ARSA** to the drug combination study in (Tian et al. 2009) using the method of Section 4.1.2. In the Introduction we mentioned that the simulation of uniformly distributed random points on the tetragon $\mathbb{P}(a_1, a_2, a_3, a_4)$ is of particular interest for the consideration of the combination study of two drugs with linear dose-response curves. Consider again the tetragonal domain $\mathbb{P}(a_0, b_0)$ in (1), the matrix A and vector b from (3) can be determined from the representation

$$\begin{aligned} \mathbb{P}(a_0, b_0) &= \{(x_1, x_2^*)^T \in \mathbb{R}^2 : -\beta_1 x_1 - \beta_2 x_2^* \le \alpha_1 - a_0, \beta_1 x_1 + \beta_2 x_2^* \le b_0 - \alpha_1, \\ &\quad - x_1 \le 0, -x_2^* \le 0\} \\ &= \left\{ \begin{pmatrix} x_1 \\ x_2^* \end{pmatrix} \in \mathbb{R}^2 : \underbrace{\begin{pmatrix} -\beta_1 & -\beta_2 \\ \beta_1 & \beta_2 \\ -1 & 0 \\ 0 & -1 \end{pmatrix}}_{=A} \begin{pmatrix} x_1 \\ x_2^* \end{pmatrix} \le \underbrace{\begin{pmatrix} \alpha_1 - a_0 \\ b_0 - \alpha_1 \\ 0 \\ 0 \end{pmatrix}}_{=b} \right\}. \end{aligned} \tag{9}$$

Now, our Algorithm 1 applies.

For a numerical illustration we consider $LY-168$ from (Tian et al. 2009) which is said to be a potential anti melanoma agent and has the single dose-response curve $f_1(x_1) = 101.91-31.17x_1$. $LY-168$ will be considered with Sorafenib which is marketed as Nevaxar by Bayer for the treatment of advanced renal cell cancer and also of advanced thyroid cancer in the USA. Its dose-response curve is given by $f(x_2) = 111.85-9.56x_2 = 101.91-9.56(x_2-1.04)$. If the chosen dose ranges from 20% to 80% and $x_2^* = x_2 - 1.04$, the experimental domain is given by

$$\mathbb{P}(20,80) = \left\{ \begin{pmatrix} x_1 \\ x_2^* \end{pmatrix} \in \mathbb{R}^2 : 20 \le 101.91 - 31.17x_1 - 9.56x_2^* \le 80, x_1 \ge 0, x_2^* \ge 0 \right\}$$

$$\underset{(9)}{=} \left\{ \begin{pmatrix} x_1 \\ x_2^* \end{pmatrix} \in \mathbb{R}^2 : \underbrace{\begin{pmatrix} 31.17 & 9.56 \\ -31.17 & -9.56 \\ -1 & 0 \\ 0 & -1 \end{pmatrix}}_{=A} \begin{pmatrix} x_1 \\ x_2^* \end{pmatrix} \preceq \underbrace{\begin{pmatrix} 81.91 \\ -21.91 \\ 0 \\ 0 \end{pmatrix}}_{=b} \right\}.$$

Since $\mathbb{P}(20,80)$ has vertices $a_1 = (0.7029195, 0)^T$, $a_2 = (2.627847, 0)^T$, $a_3 = (0, 8.567992)^T$ and $a_4 = (0, 2.291841)^T$, we can choose $Q = [0, 2.627847] \times [0, 8.567992]$ and apply Algorithm 1 with input A, b, 0, 0, 2.627847, 8.567992. Figure 7 shows the result of an acceptance-rejection simulation of uniformly distributed random points on $\mathbb{P}(20,80)$ with acceptance rates of about 46 percent.

Example 7 Let $\mathbb{P}(a_1, a_2, a_3, a_4, a_5, a_6)$ be the triangular prism with vertices $a_1 = (1,1,0)^T, a_2 = (4,1,0)^T, a_3 = (5,3,0)^T, a_4 = (3,1,3)^T, a_5 = (4,1,1)^T$ and $a_6 = (13/3, 5/3, 3)^T$. For an illustration of the triangular prism, see Fig. 8.

Here,

$$A' = \begin{pmatrix} 0 & 0 & 6 \\ 0 & -9 & 0 \\ -2 & 1 & 0 \\ -6 & 12 & 4 \\ 4/3 & -8/3 & 2/3 \end{pmatrix} \text{ and } b' = \begin{pmatrix} 0 \\ -9 \\ -7 \\ 6 \\ 10/3 \end{pmatrix}.$$

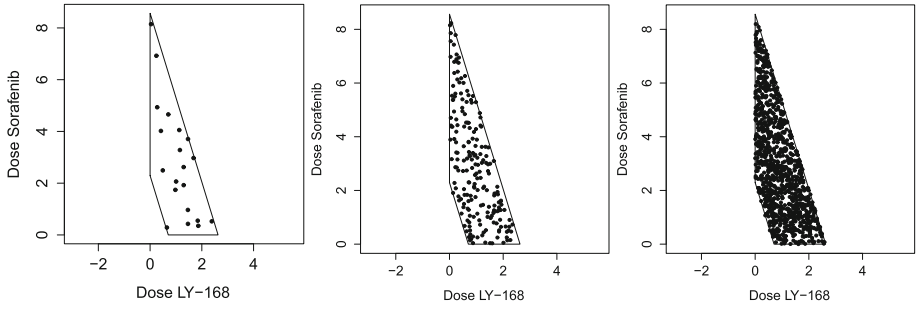

Fig. 7 20 (*left*), 200 (*middle*) and 1000 (*right*) uniformly distributed points on $\mathbb{P}(20,80)$

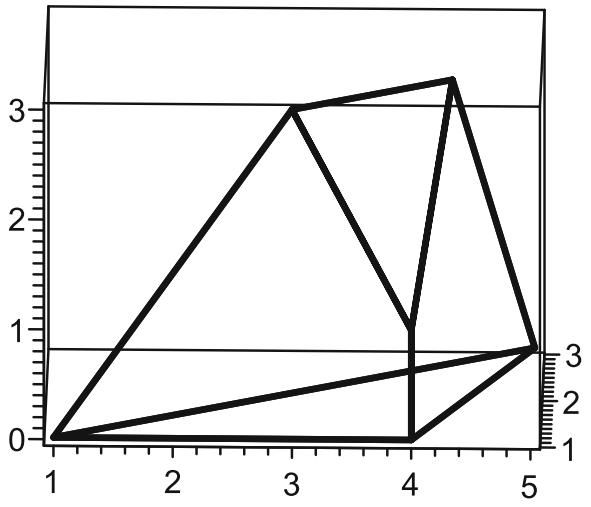

Fig. 8 Triangular prism $\mathbb{P}(a_1,\ldots,a_6)$ in Example 7

Applying Algorithm 2, it follows that

$$z_1 = \begin{pmatrix} 0 \\ -9 \\ -1 \\ 6 \\ -4/3 \end{pmatrix}, \text{thus } A_1 = \begin{pmatrix} 0 & 0 & 6 \\ 0 & -9 & 0 \\ 2 & -1 & 0 \\ -6 & 12 & 4 \\ 4/3 & -8/3 & 2/3 \end{pmatrix} \text{ and } b_1 = \begin{pmatrix} 0 \\ -9 \\ 7 \\ 6 \\ 10/3 \end{pmatrix}.$$

Moreover, $z_2 = (0,-9,7,-12,8/3)^T$, $A_2 = A_1$ and $b_2 = b_1$,
$z_3 = (0,-27,7,6,-4/3)^T$, $A_3 = A_2$ and $b_3 = b_2$,

$$z_4 = \begin{pmatrix} 18 \\ -9 \\ 5 \\ 6 \\ 10/3 \end{pmatrix}, A_4 = \begin{pmatrix} 0 & 0 & -6 \\ 0 & -9 & 0 \\ 2 & -1 & 0 \\ -6 & 12 & 4 \\ 4/3 & -8/3 & 2/3 \end{pmatrix} \text{ and } b_4 = b_3,$$

$z_5 = (-6,-9,7,-8,10/3)^T$, $A_5 = A_4$ and $b_5 = b_4$, $z_6 = (-18,-15,7,6,10/3)^T$, $A_6 = A_5$ and $b_6 = b_5$. Finally it follows, with $A = A_6$ and $b = b_6$, that $\mathbb{P}(a_1,\ldots,a_6) = \{(x,y,z)^T \in \mathbb{R}^3 : A(x,y,z)^T \le b\}$.

Example 8 Here we apply **ARSA** to the drug combination study in (Tian et al. 2009) using the method of Section 4.2.2. The simulation of uniform distributions in triangular prisms in $\mathbb{R}^3$ is required in experimental designs for the combination study of three drugs with log-linear-dose-response curves that are, according to (Berenbaum 1989) and (Tian et al. 2009), found in a wide variety of systems such as antibiotics, narcotics, cromoglycate and others. The single dose-response curves for drugs A_i, $i = 1,2,3$ are assumed to be $f_i(x_i) = \alpha_i + \beta\log(x_i)$, $i = 1,2,3$. According to (Berenbaum 1989; Tan et al. 2003; Tian et al. 2009) the additive model at the combination dose (x_1,x_2,x_3) is

$$y(x_1,x_2,x_3) = \alpha_1 + \beta\Bigg(\log(z_1) + \log((1-\rho_0)z_2 + \rho_0) + \log\left(\left(1-\frac{\rho_1}{\rho_0}\right)(1-z_3) + \frac{\rho_1}{\rho_0}\right)\Bigg),$$

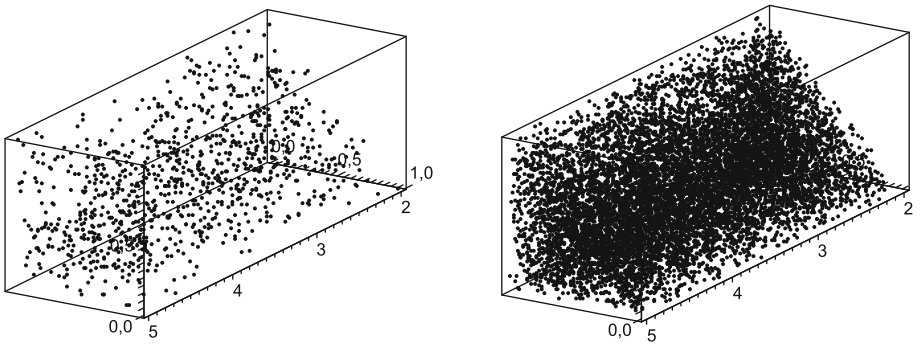

Fig. 9 Simulation of 10^3 (left) and 10^4 (right) uniformly distributed random points on $\mathbb{P}(2,5)$

where $\rho_0 = e^{(\alpha_2-\alpha_1)/\beta}$, $\rho_1 = e^{(\alpha_3-\alpha_1)/\beta}$, $z_1 = x_1 + x_2 + x_3$, $z_2 = x_1/(x_1 + x_2 + \rho_1 x_3/\rho_0)$ and $z_3 = x_3/(x_1 + x_2 + x_3)$. It is also shown there that experimental points (z_1, z_2, z_3) maximizing the statistical power in detecting synergy should be uniformly scattered in the domain

$$\mathbb{P}(z_l, z_u) = \left\{ \begin{pmatrix} z_1 \\ z_2 \\ z_3 \end{pmatrix} \in \mathbb{R}^3 : z_l < z_1 < z_u, 0 < z_2, 0 < z_3, 0 < z_2 + z_3 < 1 \right\}. \tag{10}$$

Since $\mathbb{P}(z_l, z_u)$ is a triangular prism, the methods described in Sections 4.2.1 and 4.2.2 apply to simulating uniformly distributed random points on $\mathbb{P}(z_l, z_u)$. Alternatively, we can use representation (10) to calculate A, b and Q for the application of Algorithm 1, since

$$\begin{aligned} \mathbb{P}(z_l, z_u) &= \left\{ \begin{pmatrix} z_1 \\ z_2 \\ z_3 \end{pmatrix} \in \mathbb{R}^3 : z_1 < z_u, -z_1 < -z_l, -z_2 < 0, -z_3 < 0, z_2 + z_3 < 1, \right. \\ &\qquad \left. - z_2 - z_3 < 0 \right\} \\ &= \left\{ \begin{pmatrix} z_1 \\ z_2 \\ z_3 \end{pmatrix} \in \mathbb{R}^3 : \underbrace{\begin{pmatrix} 1 & 0 & 0 \\ -1 & 0 & 0 \\ 0 & -1 & 0 \\ 0 & 0 & -1 \\ 0 & 1 & 1 \\ 0 & -1 & -1 \end{pmatrix}}_{=A} \cdot \begin{pmatrix} z_1 \\ z_2 \\ z_3 \end{pmatrix} < \underbrace{\begin{pmatrix} z_u \\ -z_l \\ 0 \\ 0 \\ 1 \\ 0 \end{pmatrix}}_{=b} \right\}. \end{aligned}$$

Furthermore, the boundaries of $\mathbb{P}(z_l, z_u)$ can be read out off representation (10). Thus Q can be chosen as $Q = [z_l, z_u] \times [0,1] \times [0,1]$. For an illustration, we refer to Fig. 9, where 1000 and 10000 uniformly distributed random points are simulated on $\mathbb{P}(2,5)$.

Acknowledgement
The authors are grateful to a referee who provided valuable suggestions on improving the paper and an additional recent reference, and declare that they have no competing interests in the paper.

Received: 14 November 2016 Accepted: 21 February 2017
Published online: 21 March 2017

References

Arnold, B, Castillo, E, Sarabia, JM: Multivariate distributions defined in terms of contoures. J. Stat. Plan. Infer. **138**, 4158–4171 (2008)

Avis, D: lrs: A Revised Implementation of the Reverse Search Vertex Enumeration Algorithm. Birkhäuser Verlag, Basel (2000). doi:10.1007/978-3-0348-8438-9_9

Balkema, G, Embrechts, P, Nolde, N: Meta densities and the shape of their sample clouds. J Multiv Analysis. **101**(7), 1738–1754 (2010)

Berenbaum, MC: What is synergy? Pharmacol. Rev. **41**(2), 93–141 (1989)

Böhm, J, Hertel, E: Mathematische Monographien: Polyedergeometrie in n- dimensionalen Räumen konstanter Krümmung, vol 14. VEB Deutscher Verlag der Wissenschaften, Berlin (1980)

Cutler, B, Dorsey, J, McMillan, L: Simplification and improvement of tetrahedral models for simulation. In: The 2004 Eurographics/ACM SIGGRAPH Symposium on Geometry Processing, pp. 93–102. ACM, New York, (2004)

Fang, KT, Yang, ZH: On uniform design of experiments with restricted mixtures and generation of uniform distribution on some domains. Stat. Probab. Lett. **46**, 113–120 (2000)

Fang, KT, Kotz, S, Ng, KW: Monographs on Statistics and Applied Probability: Symmetric Multivariate and Related Distributions, vol 36. Chapman & Hall, New York (1990)

Fernandez, C, Osiewalski, J: Steel, MFJ: Modeling and inference with ν-spherical distributions. J Am. Stat. Assoc. **90**, 1331–1340 (1995)

Fukuda, K, Prodon, A: Double Description Method Revisited. In: Combinatorics and Computer Science. Springer- Verlag, Berlin, Heidelberg, (1996). doi:10.1007/3-540-61576-8_77

Gupta, A, Song, D: l_p-norm spherical distribution. J. Stat. Plann. Infer. **60**(2), 241–260 (1997)

Henschel, V, Richter, W-D: Geometric generalization of the exponential law. J. Multivar. Anal. **81**, 189–204 (2002). doi:10.1006/jmva.2001.2001

Kalke, S, Richter, W-D: Simulation of the p- generalized gaussian distribution. J. Stat. Comput. Simul. **83**(4), 641–667 (2013). doi:10.1080/00949655.2011.631187

Kamiya, H, Takemura, A, Kuriki, S: Star-shaped distributions and their generalizations. J. Stat. Plan. Infer. **138**, 3429–3447 (2008)

von Neumann, J: Various techniques used in connection with random digits.monte carlo methods. Nat. Bureau Standards. **12**, 36–38 (1951)

Nolan, J: An R package for modeling and simulating generalized spherical and related distributions. J. Stat. Distrib. Appl. **3:14**, 11 (2016)

Richter, W-D: Eine geometrische Methode in der Stochastik. Rostocker Mathematisches Kolloquium. **44**, 63–72 (1991)

Richter, W-D: Continuous $l_{n,p}$- symmetric distributions. Lith. Math. J. **49**(1), 93–108 (2009). doi:10.1007/s10986-009-9030-3

Richter, W-D: Geometric and stochastic representations for elliptically contoured distributions. Commun. Stat. Theory Methods. **42**, 579–602 (2013). doi:10.1080/03610926.2011.611320

Richter, W-D: Geometric disintegration and star- shaped distributions. J. Stat. Distrib. Appl. **1:20**, 24 (2014). doi:10.1186/s40488-014-0020-6

Richter, W-D: Convex and radially concave contoured distributions. J. Probab. Stat. **2015**, 12 (2015a). doi:10.1155/2015/165468

Richter, W-D: Norm contoured distributions in $\mathbb{R}^2$. Lect. Notes Seminario Interdisciplinare di Matematica. **12**, 179–199 (2015b)

Richter, W-D, Schicker, K: Ball numbers of platonic bodies. J. Math. Anal. Appl. **416**(2), 783–799 (2014). doi:10.1016/j.jmaa.2014.03.007

Richter, W-D, Schicker, K: Polyhedral star-shaped distributions. J. Probab. Stat. **2017**, 35 (2017)

Rocchini, C, Cignoni, P: Generating random points in a tetrahedron. J. Graphics Tools. **5**(4), 9–12 (2000)

Sarabia, JM, Gomez-Deniz, E: Construction of multivariate distributions: a review of some results. SORT. **32**(1), 3–36 (2008). With discussion by Pardo, M.C., 39-42 and Navarro, J., 43-46

Tan, M, Fang, HB, Tian, GL, Houghton, PJ: Experimental design and sample size determination for testing synergism in drug combination studies based on uniform measures. Stat. Med. **22**, 2091–2100 (2003). doi:10.1002/sim.1467

Tian, GL, Fang, HB, Tan, M, Qin, H, Tang, ML: Uniform distributions in a class of convex polyhedrons with applications to drug combination studies. J. Multivariate Anal. **100**, 1854–1865 (2009). doi:10.1016/j.jmva.2009.02.011

Ziegler, GM: Lectures on Polytopes. Springer-Verlag, Berlin, Heidelberg (1995)